

A Dataset for Provident Vehicle Detection at Night

Sascha Saralajew,^{*,1} Lars Ohnemus,^{*,2} Lukas Ewecker,^{*,2} Ebubekir Asan,^{*,2} Simon Isele,² and Stefan Roos²

Abstract—In current object detection, algorithms require the object to be directly visible in order to be detected. As humans, however, we intuitively use visual cues caused by the respective object to already make assumptions about its appearance. In the context of driving, such cues can be shadows during the day and often light reflections at night. In this paper, we study the problem of how to map this intuitive human behavior to computer vision algorithms to detect oncoming vehicles at night just from the light reflections they cause by their headlights. For that, we present an extensive open-source dataset containing 59 746 annotated grayscale images out of 346 different scenes in a rural environment at night. In these images, all oncoming vehicles, their corresponding light objects (e.g., headlamps), and their respective light reflections (e.g., light reflections on guardrails) are labeled. In this context, we discuss the characteristics of the dataset and the challenges in objectively describing visual cues such as light reflections. We provide different metrics for different ways to approach the task and report the results we achieved using state-of-the-art and custom object detection models as a first benchmark. With that, we want to bring attention to a new and so far neglected field in computer vision research, encourage more researchers to tackle the problem, and thereby further close the gap between human performance and computer vision systems.

I. INTRODUCTION

Object detection is one of the most popular and best studied fields in computer vision. One reason is that object detection is essential to several applications, for example, autonomous driving and surveillance cameras. Currently, State-Of-The-Art (SOTA) object detection is performed by Neural Networks (NNs) and the target is to predict Bounding Boxes (BBs) that describe the position of *visible* objects. Thereby, a not negligible restriction is the visibility assumption in form of direct sight to objects (ignoring systems that combine detection and tracking to deal with occluded objects). In contrast, in certain situations, human perception is capable to reason about the position of objects without direct visibility—for instance, by considering the illumination changes in an environment at daylight (e.g., in form of shadow movements). When driving a car at night, a similar human ability becomes a key feature for safe and anticipatory driving: The ability to reliably detect light reflections in the environment caused by the mandatory headlamps of other road participants. Building on this ability, drivers can predict other vehicles and their position, in the sense where the object will occur in the future, even though they are *not* in direct sight.

^{*} Authors contributed equally.

¹Bosch Center for Artificial Intelligence, Renningen, and Leibniz University Hannover, Institute of Product Development, Hannover, both Germany. The research was performed during employment at Dr. Ing. h.c. F. Porsche AG. sascha.saralajew@bosch.com

²Dr. Ing. h.c. F. Porsche AG, Weissach, Germany. [lars.ohnemus1, lukas.ewecker, ebubekir.asan}@porsche.de](mailto:{lars.ohnemus1, lukas.ewecker, ebubekir.asan}@porsche.de)



Fig. 1. Annotation of light artifacts with KPs (dots) and the corresponding inferred saliency maps (colored areas represent the saliency of one KP).³

Motivated by the aforementioned human provident behavior and the discrepancy to SOTA object detection, we provide with this paper all the tools needed to boost “ordinary” vehicle detection at night to provident vehicle detection such that consumer products can take advantage of this ability soon. To this end, we introduce and publish⁴ an annotated image dataset containing 346 different sequences with 59 746 annotated grayscale images in total captured at two different exposures. Each image is equipped with several annotations—in form of KeyPoints (KPs)—that describe the position of other vehicles and all their produced light instances (effects). Exemplary, we use this dataset to train several machine learning models to detect light reflections that might serve as baselines for future research. In order to properly evaluate object detectors on the proposed dataset, we discuss commonly used evaluation metrics in object detection and propose specially crafted metrics for the dataset. Beyond the presented application of provident vehicle detection at night, the structure of the dataset is carefully designed such that it will be useful for other investigations as well (e.g., object tracking at night, transfer learning between different image exposure cycles).

The outline of the paper is as follows: In the next section, we discuss related work. Following this, we describe the annotation methodology and the challenges in annotating light reflections. With these insights, Section IV explains the process of creating the Provident Vehicle Detection at Night (PVDN) dataset. Afterwards, Section V shows the versatility of our annotation strategy by extending the dataset with saliency- and BB-representations. To analyze the performance of detectors on the dataset, we craft evaluation metrics in Section VI. After that, we present benchmark models trained on the dataset and finish with a conclusion and discussion.

³All images are brightness adjusted, cropped to the region of interest, and best viewed when printed in color.

⁴<https://www.kaggle.com/saralajew/provident-vehicle-detection-at-night-pvdn>

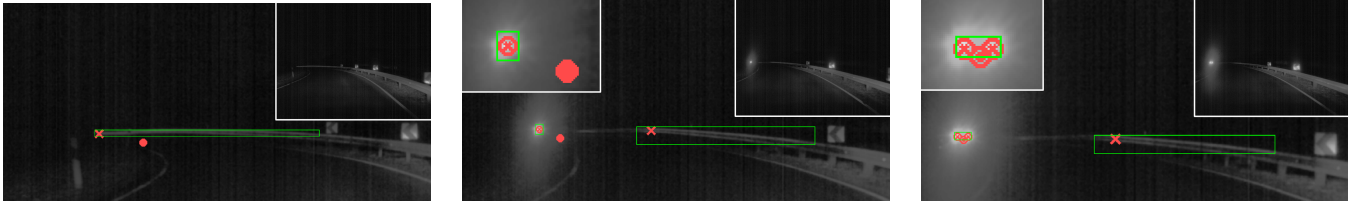


Fig. 2. The three characteristic detection states in an example scene (number 309) with the following annotations: indirect vehicle position KPs (dot), direct vehicle position KPs (circle-dot), indirect instance KPs (cross), direct instance KPs (circle-cross), and automatically inferred BBs. Each visualization shows a cropped area of the entire image (shown in the upper right corner). If necessary, the left upper corner shows a second crop of the area of interest. Left: First visible light reflections at the guardrail. Middle: First direct sight to the vehicle. Right: Full direct sight to the vehicle.

II. RELATED WORK

Due to their broad application for driver assistance systems (e. g., automatic high beam control), the detection of vehicles at night is well-studied. Current SOTA detectors detect vehicles by their visible headlamps and rear lights [1], [2], [3], [4], [5], [6] so that these detection systems are limited to the detection of visible vehicles solely. Therefore, published datasets alongside these papers focus on the annotation of headlamps and rear lights (see also [7]).

Oldenzien et al. [8] studied the deficit between the human provident vehicle detection and a driver assistance system camera-based vehicle detection system. Based on a test group study, they showed that drivers detected oncoming vehicles on average 1.7 s before the camera system, which is a not negligible time discrepancy. Later in their work, they used a Faster-RCNN architecture [9] to detect light reflections caused by other vehicles. For this purpose, they crafted a dataset (~700 images) by annotating light reflections and headlamps with BBs. Even if the NN was able to learn the task to some extent, they questioned whether BB annotations are the correct annotation method since the absence of clear boundaries of light reflections caused a high annotation uncertainty.⁵

Orthogonal to the presented work here, Naser et al. [10] analyzed shadow movements to providently detect objects at daylight. For that, they assumed that the ground plane is fixed and known to analyze consecutive image frames by their homography. Due to this assumption, their framework is not applicable to providently detect vehicles at night.

III. ANNOTATION METHODOLOGY

Usually, creating a dataset for object detection is straightforward: Objects inside images are annotated by placing BBs around them. Therefore, each BB directly specifies the image region that is taken up by an object. Together with a class label, this perfectly specifies the object. This, however, is not true for the task of provident detection since, inherently, there is no image region associated with the object we want to detect. Therefore, we have to deduce the existence of oncoming cars by studying light artifacts in images. Unlike ordinary object detection, light artifacts present several challenges due to their fuzzy nature, abundance of light reflections, and glare. It gets even more complicated when, in a realistic scene with multiple oncoming vehicles and

other light sources such as streetlights, we need to match the light artifacts to their sources in order to infer correctly. So, while the overall goal—detecting oncoming vehicles early—is easy to state, the precise definition of the methodology to derive a suitable dataset is more complicated.

A. Annotation of Vehicle Positions

The annotation of an approaching vehicle poses two challenges:

- 1) How to represent the position within a frame, and
- 2) where to place the vehicle position when it is not in direct sight?

When the vehicle is in direct sight, the most efficient way to annotate the position is to place a KP at a remarkable point on the vehicle. Placing a KP on the road centrally between both headlights perfectly specifies the vehicle’s position—see the right image in Fig. 2. The choice of assigning a BB to the vehicle might seem to be more natural but can be made redundant when the headlights of the vehicle are marked by KPs as well. A robust BB can then be always inferred from the vehicle position and the two headlight KPs by taking the enveloping rectangle of all three KPs.

Stringently, the predicted position of not yet visible vehicles—we will call them *indirectly* visible—can be annotated with a KP as well. With possible prediction algorithms in mind, this KP is placed at the location of the first sight of the approaching vehicle: the end of the visible road (if the road touches the edge of the image, the intersection point is used)—see Fig. 2 (left and middle) for an illustration. This approach has the key advantages that it conserves temporal coherence when transitioning between indirect and direct vehicle positions; and that the KP can be directly used as a target when predicting the occurrence position of vehicles.

Future systems might need to make different decisions depending on whether it is a directly or indirectly visible vehicle. To ease this, a Boolean label is added to each vehicle position to specify whether it is directly or indirectly visible.

B. Notations and Annotation Hierarchy

Generally, for annotation, we study image sequences (scenes) showing the scenario “approaching vehicle at night”. Within such scenes, vehicles are detected. Since the *vehicle position* is also an abstract notion for not directly visible vehicles, the presence of vehicles might be predicted through light artifacts within a frame. To emphasize this relationship,

⁵Note that this paper is a continuation of this earlier work by our team.

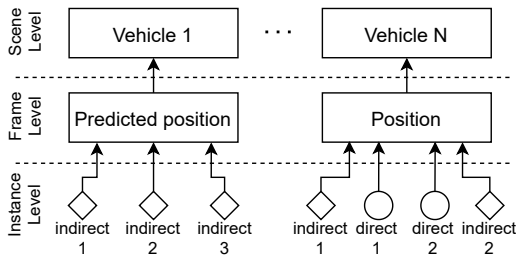


Fig. 3. Hierarchy of different entities used for the PVDN dataset. The structure allows for multiple vehicles each having a single (predicted) position. The vehicles are observed through a variable number of instances.

we denote any form of light artifacts as an *instance* of the vehicle. The “human” approach to predict and detect vehicles at night spans three hierarchical semantic levels. On the top level—the *scene level*—the aim is to predict and locate oncoming vehicles. This usually uses both temporal and spatial features. While the consideration of consecutive frames allows the driver to increase the detection certainty, oncoming vehicles can be detected using isolated, single images only. On this *frame level*, the vehicles have to be located. As instances build up the knowledge about vehicles, they are placed on the lowest semantic level, the *instance level*. The instances are essential because, for not directly visible vehicles, they are the only features available to infer the vehicles’ positions. Fig. 3 shows the hierarchy that implies two requirements for a suitable annotation strategy:

- 1) vehicle positions and their instances must be annotated;
- 2) annotations should be coherent over multiple frames to capture the temporal characteristics.

While the second requirement can be enforced by assigning IDs to each annotated entity, the annotation of vehicle positions and instances requires further investigations.

C. Annotation of Instances

We split the annotations in the same way we did for the vehicle position. Instances can be both direct (headlights) or indirect (halos, reflections), see Fig. 2. While direct instances are well-specified, the total number and size of the indirect instances cannot be specified objectively. The headlights might bounce and be reflected multiple times, leaving instances of various strengths all around the image.

1) *Lessons learned of BB annotations:* Oldenziel et al. [8] used BBs to represent light reflections, as already stated in Section II, and noticed a strong tendency of the detector towards False Positive (FP) detections. We hypothesize, that this was mainly caused by two reasons: First, only the strongest light artifact was annotated to represent a vehicle. Even if this assumption resulted in an objective annotation strategy, it seemed to confuse the system as the intensity of the strongest instance is always dependent on the entire scenario. Thus, a lot of predictions might be True Positives (TPs) but were considered FPs due to the missing annotations of weaker instances. Second, the metric used for evaluating predictions—the Intersection over Union (IoU)—is sensible to size variations between ground truth and predictions. While

this is usually desired for object detection, it requires a well-specified, objective ground truth. However, on many occasions, both the ground truth and the prediction could be considered correct while still giving a small IoU. This poses the question: Is it possible to objectively specify BBs? To address this, we performed a small experiment, tasking multiple experts to annotate the same indirect instance with BBs. The results show that on average the experts’ BBs only overlapped with a median IoU of 59.4% for the indirect instance. This effect is even worse for direct instances, resulting in a median IoU of just 52.0%. For a more detailed discussion of the annotation experiment, see Appendix I.

2) *KP annotations based on saliency:* Based on the previous discussion, it is clear that a proper annotation strategy should not insinuate the existence of perfect annotations and therefore leading to false conclusions on the real problem. Thus, a suitable strategy has to be flexible enough to allow for variations while still describing the situation properly. Simply put, the annotation strategy should be guided by the local light intensity because this is the only available feature to judge the existence of instances. In real life, such local light intensities or locally *salient regions* attract the attention of drivers, and the goal of the annotation process is to mimic this attention behavior.

An approach to this attention behavior is to mark points of high visual saliency by KPs without proclaiming a boundary, see Fig. 2. With these KPs carefully placed in salient regions, we have markers for human attention—similar to datasets using eye-fixation points as descriptors of visual saliency [11]. This annotation approach captures the top-down aspect of human attention [12], which is goal-driven (detect oncoming vehicles). After the annotation, we can use the KPs to check for intensity stimuli that lead the annotators to the decision to place a KP in this region, which corresponds to a bottom-up or stimuli-based saliency approach [12]. Such a bottom-up saliency approach can be realized by comparing the pixel intensities of the surrounding area with the intensity value at the KP. Usually, the intensity values in the surrounding area are on average slightly lower than the KP intensity because the annotators intuitively look at the most salient point first—the intensity maximum. In Fig. 1 we show an example where the salient region was inferred from the KP (see Section V for further details about the saliency inference). Using this approach, we can specify entire instances without stating ground-truth borders but rather suggestions of interesting image regions. Additionally, the approach is fairly robust to variations in the KP placement.

This annotation strategy applies to direct and indirect instances. For direct instances, the KP is placed centrally within the headlight cone, see Fig. 2. To distinguish between both instance types, we add a Boolean label. Additionally, it is worth noting, that this strategy is efficient to carry out since only one point per instance has to be annotated.

IV. THE PVDN DATASET

The PVDN dataset is derived from a test group study performed to analyze provident vehicle detection skills of

TABLE I
TRAINING-VALIDATION-TEST SPLIT OF THE PVDN DATASET.

	exposure	#scenes	#images	#veh.-pos.	#instances
train	day	113	19 078	15 403	45 765
	night	145	25 264	26 615	72 304
val	day	20	3 898	2 602	7 244
	night	25	4 322	3 600	12 746
test	day	19	3 132	3 045	9 338
	night	24	4 052	3 384	10 438
total	day	152	26 108	21 050	62 347
	night	194	33 638	33 599	95 488
	cumulated	346	59 746	54 649	157 835

humans [8]. During the study, the onboard camera of the test car was used to capture grayscale images of two different exposure cycles (each at 18Hz). The resulting image cycles are called “day cycle” (short exposure) and “night cycle” (long exposure). Image sequences (scenes, available through the test group study) are selected according to the appearance of oncoming vehicles and padded to create parts without vehicles in them. Mostly, such sequences begin when there is no sign of the oncoming vehicle and end when the vehicle has passed. For each sequence either the day or the night cycle is annotated according to the methodology described in Section III.

As already mentioned, the annotation of indirect instances and vehicle positions is subjective. To minimize the subjectivity effects, an iterative procedure for the annotation process was chosen. KPs for vehicle position and instances were annotated with a custom annotation tool.⁶ Then, the annotations were reviewed by multiple annotators and the placement and number of KPs was discussed. Additionally, a set of guidelines for different conditions and circumstances was given to the annotators. The reviewed annotations were then corrected by an annotator.

The dataset contains 59 746 annotated images, spread over 346 scenes. In comparison to the Enz-dataset [8], the share of indirect instances to direct instances is balanced (ca. 49% of instances are indirect). The same is true when considering vehicle positions (43% of the annotated vehicle positions are indirect). The total numbers of scenes, images, vehicle positions, and instances are summarized in Table I.

V. EXTENDING THE INSTANCE ANNOTATIONS

While KP annotations allow for a compact and natural annotation strategy, they are not commonly used in object detection. Therefore, we provide automated approaches to regress salient regions from the instance KPs, representing them with both saliency maps and BBs.

A. Generation of Saliency Maps

We use a modified version of the Boolean Map Saliency (BMS) method introduced by Zhang and Sclaroff [13] to

⁶<https://github.com/larsOhne/pvdsn>

automatically generate saliency maps. In the original approach, saliency was deduced by thresholding image channels. The resulting Boolean maps are then filtered using the assumption that salient regions are not connected to the image borders (center-surround antagonism) and averaged to retrieve attention maps. However, the center surround-antagonism does not hold for the PVDN dataset because the instances are in general not centered within the image. Thus, we replaced the original criterion with a KP-centered approach.

To retrieve saliency maps for the PVDN dataset, we apply a flood fill algorithm with the KPs as seed pixels for the filtering in the Boolean maps. Additionally, we improve the original BMS method by restricting the maximal threshold value to approximately 1.2 times the KP intensity because otherwise, the salient region might leak into other high-intensity regions. In Fig. 1, we show an exemplary salient region around a KP generated with this modified BMS method.

Given a KP $\tilde{\mathbf{p}}$, the corresponding saliency map $s(\mathbf{p} | \tilde{\mathbf{p}})$ assigns each pixel $\mathbf{p} \in I$ in the image I a saliency value $s : I \rightarrow [0, 1]$. The saliency maps across all KPs can be used to directly learn end-to-end saliency-based object detectors (e.g., using methods described by Borji et al. [14]) or can be used to improve KP metrics, see Section VI.

B. Generation of Bounding Boxes

There are the following two options to generate BBs for the PVDN dataset:

- use the KPs to filter predictions of a BB regressor;
- regress BBs directly from the local intensities and KPs.

For filtering, we assume that a suitable system generated a list of candidate BBs. Then, we validate each of these candidate BBs by checking whether at least one KP is contained inside the BB. If there is, we consider the BB a TP. Otherwise, the BB is considered a true negative.

One possible candidate generation we will use later in the paper is based on the adaptive binarization approach proposed by Singh et al. [15]. This method efficiently determines binary masks of images where blobs are highlighted by computing a locally adaptive binarization threshold based on local means and mean deviations. Each blob is then converted into a BB by computing the enclosing rectangle of the connected region. In Fig. 4, the first three steps visualize the candidate generation and Fig. 2 shows example TP BBs.

The other approach to generate BBs is similar to the saliency approach and uses simple thresholding around the KP intensities to generate a Boolean map. In this Boolean map, we filter the instance blobs by applying a blob detection algorithm with the KPs as seeds. Analogously, binarization thresholds can be chosen relative to the KP intensities, which makes the BBs more robust for weak instances. A more detailed analysis of the BB generation is provided in [16].

VI. EVALUATION METRICS

To properly evaluate object detection methods on the PVDN dataset, we provide specially crafted evaluation metrics for BB and KP predictors.

A. Evaluation Metric for Bounding Box Predictors

As explained in Section V-B, it is possible to infer BBs from the KP annotations. To enable the use of current SOTA object detection methods—that usually predict BBs—on the PVDN dataset, we provide a metric to evaluate their performance based on the ground truth KPs. Without loss of generality,⁷ we define the evaluation method for binary BB predictors. Hence, the task is to determine whether a BB corresponds to an instance (either direct or indirect).

When detecting and classifying objects via BBs, the most common metrics to evaluate model performance are mean Average Precision (mAP) and mean Average Recall (mAR). For both, the match between a ground truth BB and a predicted BB is determined by calculating the Intersection over Union (IoU). If the IoU between a ground truth and predicted BB exceeds a certain threshold, both are considered a match and the classification performance can be determined by comparing the ground truth and predicted label. Obviously, determining the correspondence of ground truth and predicted BBs via IoU is only feasible if the ground truth annotations provide BBs. Since the instances in the PVDN dataset are annotated via KPs, calculating the IoU is not possible. In this case, our proposed metric to compare predicted BBs with ground truth KPs follows the idea that

- each BB should span around exactly one KP, and
- each KP should lie within exactly one BB.

Consequently, it should be quantified when *a*) a BB contains no KP, *b*) a BB contains more than one KP, *c*) a KP does not lie within any BB, and *d*) a KP lies within more than one BB.

First, to compute precision and recall in the usual manner, to quantify *a*) and *c*), we introduce the following events:

- True Positive (TP): The instance is described (at least one BB spans over the KP);
- False Positive (FP): The BB describes no instance (no KP lies within the BB);
- False Negative (FN): The instance is not described (no BB spans over the KP).

Second, to quantify the BB quality of TP events, we calculate the following quantities:

- The number of KPs in a BB b that is a TP, denoted by $n_K(b)$;
- The number of BBs that are TPs and that cover a described KP k , denoted by $n_B(k)$.

These numbers are converted into measures in the range $[0, 1]$, where one means best quality, and averaged across the dataset by

$$q_K = \frac{1}{N_B} \sum_b \frac{1}{n_K(b)}$$

and

$$q_B = \frac{1}{N_K} \sum_k \frac{1}{n_B(k)}.$$

⁷The evaluation can be extended to multiple classes (e. g., direct instance, indirect instance, and no instance). However, defining it as a binary problem avoids the task to resolve ambiguities (when a BB contains a direct KP and an indirect KP).

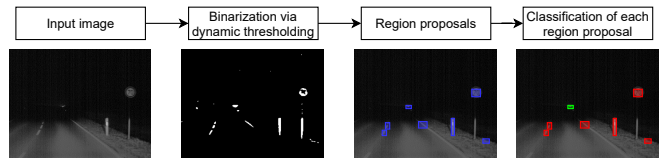


Fig. 4. Architecture overview of the custom model.

Thereby, N_B is the total number of BBs that are TPs and N_K is the total number of described KPs. These measures quantify the uniqueness of BBs with respect to *b*) and *d*). For example, in an image with several KPs, q_k is low if a large BB spans over the whole image, since it will then capture several KPs and the term $\frac{1}{n_K(b)}$ decreases. The overall quality is determined by $q = q_K \cdot q_B$.

B. Evaluation Metric for Keypoint Predictors

Instead of predicting BBs, another option to solve the problem is to predict KP coordinates for each instance. Usually, KP prediction tasks evaluate methods also by calculating mAP and mAR but determining the correspondence of ground truth to prediction not via IoU but a KP similarity measure. Inspired by the “object keypoint similarity” method⁸ proposed in the COCO [17] KP detection challenge, we propose a way to measure KP similarity, denoted by $\text{kps}(\cdot, \cdot)$. In particular, for the PVDN dataset, we measure the similarity between a ground truth KP and a predicted KP by

$$\text{kps}(\mathbf{p}, \tilde{\mathbf{p}}) = \exp(-\|\mathbf{p} - \tilde{\mathbf{p}}\|_E \cdot |s(\mathbf{p} | \tilde{\mathbf{p}}) - s(\tilde{\mathbf{p}} | \mathbf{p})|),$$

where $\tilde{\mathbf{p}}$ refers to the pixel coordinate vector of a ground truth KP and \mathbf{p} refers to the pixel coordinate vector of a predicted KP. The function $s(\mathbf{p} | \tilde{\mathbf{p}})$ returns the saliency at the position \mathbf{p} with respect to the saliency map of the ground truth KP $\tilde{\mathbf{p}}$, see Section V-A. With this measure, the ambiguity of the ground truth KPs is addressed by scaling the Euclidean distance between the predicted and ground truth KP by the difference of the saliencies at both positions. Following the idea that an instance is annotated with a KP placed on its intensity—and therefore saliency—maximum objectively, the Euclidean distance between ground truth and predicted KP is scaled down the more similar the saliency is. This takes into account the noisy nature of the ground truth. Once the similarity score is calculated for each combination of predicted KP and ground truth KP, the optimal assignment between the prediction and ground truth is calculated by formulating the problem as finding a bipartite matching with a maximal similarity score. This problem can be efficiently solved by the Hungarian method. Having this optimal assignment, mAP and mAR can be calculated as usual.

VII. BENCHMARK EXPERIMENTS

SOTA object detection methods usually predict BBs. Although the dataset is annotated with KPs, our benchmark studies at this point focus on predicting BBs for two reasons.

⁸<https://cocodataset.org/#keypoints-eval>

TABLE II
MODEL RESULTS ON THE PVDN DATASET DETERMINED BY THE METRICS PROPOSED IN SECTION VI ON THE DAY-TEST DATASET.

Model	Input size	Parameters [M]	GFLOPs	Runtime [ms]	Precision	Recall	F-score	q	q_K	q_B
YoloV5x	960 × 960	87.2	217.1	28.1	1.00	0.68	0.81	0.37	0.38 ± 0.20	0.98 ± 0.08
YoloV5s	960 × 960	7.1	16.4	14.8	0.99	0.66	0.80	0.37	0.38 ± 0.20	0.98 ± 0.09
Custom	480 × 640	0.9	1.6 ± 0.7	20.6 ± 3.5	0.88	0.54	0.67	0.40	0.40 ± 0.22	1.00 ± 0.00
	Generated BB day-test dataset				1.00	0.69	0.81	0.42	0.42 ± 0.24	1.00 ± 0.00

First, we want to show that based on the KP annotations the derived BBs, see Section V-B, can serve as a useful training basis. Second, SOTA KP prediction methods (e. g., [18], [19], [20]) cannot be applied out of the box without greater architecture adjustments because of

- the inherently noisy nature of the instance annotations via KPs, and
- the non-fixed number of KPs per vehicle and frame.

In a proof-of-concept, we investigated the applicability of KP predictors. However, the results were not satisfying and far behind the results of BB methods. Therefore, we decided to focus on BB-based object detection in this study. The source code of the experiments is publicly available.⁶

A. Model architectures

We evaluated three models: YoloV5x, its lightweight version YoloV5s,⁹ and a customized approach, denoted as Custom. A more detailed analysis of this approach is presented by Ewecker et al. [16]. The YoloV5 architecture was formalized to predict instance BBs (either direct or indirect). The Custom architecture is a combination of a rule-based region proposal module and a Convolutional NN (CNN) classifier—see Fig. 4 for the architecture overview and Table III in the appendix for the layer structure of the CNN. In the first step of the Custom architecture, we generate BB candidates (see the next section for details). These generated BBs, are used to crop image patches from the input image. Thereby, the cropped region has twice the size of the given BB in order to include additional context information. In the second step, the image patches are resized to 64 × 64 pixels and fed into the binary CNN classifier. The task of this classifier was to assign the label positive (instance) or negative to the BBs.

B. Evaluation Setup and Training

All evaluations are implemented in Python and C++. The NNs are implemented in PyTorch [21] and are executed on an NVIDIA Tesla V100 GPU. The main Python process and the C++ parts are running on a Intel Core i7-6850K 3.60GHz CPU.

We took the *day exposure* subset and followed the proposed adaptive thresholding method of Section V-B to generate the BBs. For this purpose, we resized the images to half the size and tuned all available hyperparameters by a random search on the validation split. After that, we used the BB regressor also as the region proposal method for the Custom

architecture. All the NNs were trained on the training split for at most 500 epochs until convergence. The final models were then selected based on the maximum F-score on the validation set over all epochs and results are reported on the test set. These evaluations were done with respect to the evaluation measures proposed in Section VI-A. Besides model performance, we also report the number of parameters and the computational complexity in terms of Giga Floating Point Operations (GFLOPs) per image as a hardware-independent measure. Additionally, model runtimes are given. If available, we report standard deviations (mean ± std).

C. Results

The numerical results are summarized in Table II. At first, we evaluated the quality of the generated ground truth BBs. Note that, in the best case, all of the performance metrics give a score of 1.0. As expected, the generated BBs yield a perfect precision of 1.0 as they naturally do not contain any FPs. However, they only provide a recall of 0.69 indicating that several KP annotations do not correspond to any BB (FN). The analysis of these errors shows that they are caused when the annotated instances have a very low saliency such that they are ignored by the adaptive thresholding. Furthermore, a box quality of 0.42 reveals that the applied method of generating BBs based on the KP annotations still has difficulties in separating instances from each other. This means that when instances are close to each other the intensity difference is not sufficient for the adaptive thresholding to distinguish the blobs and, therefore, to create object boundaries. In such cases, instances, which are annotated separately, are being described by one BB (e. g., see the right image in Fig. 2).

The best performance in terms of the F-score is achieved by the YoloV5 versions and these results are close to the scores of the generated BBs. Of course, as the learning scheme is supervised, the scores should not exceed the scores evaluated on the training data. With respect to the recall and the bounding box quality, the scores suggest that the YoloV5 was able to learn or approximate the BB generation approach that we have used for the dataset generation, which is a remarkable result. Behind the scores of the YoloV5 versions is the Custom approach with a non-trivial result, which shows that it is possible to solve this task by a combination of a rule-based and learned approach.

In terms of memory and computational complexity, the Custom approach is significantly superior to the YoloV5 versions. However, in contrast to the computational complexity, the Custom method is not faster (runtime) than the YoloV5s. The reason for that is that the C++ implementation of the BB

⁹<https://github.com/ultralytics/yolov5>

generation is not highly optimized. To put this into numbers, from the total computation time on average only 2.5 ms are required to compute the classification outputs of the CNN per image (including data loading to the GPU).¹⁰

Overall, our results show that *a*) it is possible to detect oncoming vehicles based on their light reflections and *b*) based on the KP annotations BBs can be generated that can serve as training data.

Finally, a rationale for the design of the Custom approach: We used the Custom method together with a tracking and plausibility algorithm to test prototype driver assistance functions in a test car. For that, we ran the Custom approach together with all the other applications (receiving inputs, sending outputs, etc.) in real time (faster than 18 Hz). The usage of a shallow CNN together with a rule-based BB generator has the advantage to be more transparent. Therefore, the model behavior and, especially, exceptional cases can be better understood, analyzed, and interpreted making the approach easier to validate and verify.

VIII. CONCLUSION AND OUTLOOK

Based on the work of Oldenziel et al. [8], we presented a thoroughly designed image dataset including evaluation metrics and benchmark results to investigate the problem of provident vehicle detection at night. In general, the task to providently detect objects based on visual cues is a promising new research direction to bring object detection towards human performance. With the presented work here and the open-sourcing of all data and code, we hope to provide the research community a jump start.

The annotation of light artifacts is challenging compared to ordinary object annotation due to the lack of clear object boundaries. We tackled this difficulty by an annotation approach based on placing KPs in salient regions and methods to automatically extend the base annotations to saliency maps or BBs. Even if we showed in a set of benchmark experiments that automatically generated BBs can be used to train SOTA object detectors such that they detect light reflections, the generation approach and their inherent quality is of course a limiting factor. Since we already provided an evaluation metric for KP detectors, we plan to develop KP and saliency detection methods to overcome this limiting factor.

Besides, we annotated the vehicle positions so that the PVDN dataset provides ground truth for several research fields:

- Time estimation: Time until vehicle appearance;
- Tracking: Track instances and vehicles across scenes;
- Transfer learning: Transfer methods to different exposure cycles or weather conditions (snow, rain, fog, etc.);
- Learning with label noise: Design methods that properly handle the KP or generated annotations.

We are looking forward to all the upcoming results.

¹⁰Note that the computational complexity of the Custom approach is not constant as the runtime of the proposal generation depends on the number of positive values in the Boolean map.

REFERENCES

- [1] A. López, J. Hilgenstock, A. Busse, R. Baldrich, F. Lumbreras, and J. Serrat, "Nighttime vehicle detection for intelligent headlight control," in *Advanced Concepts for Intelligent Vision Systems*, ser. Lecture notes in Computer Science, J. Blanc-Talon, S. Bourennane, W. Philips, D. Popescu, and P. Scheunders, Eds. Springer, 2008, pp. 113–124.
- [2] P. Alcantarilla, L. Bergasa, P. Jiménez, I. Parra, D. Fernández, M.A. Sotelo, and S.S. Mayoral, "Automatic lightbeam controller for driver assistance," *Machine Vision and Applications*, pp. 1–17, 2011.
- [3] S. Eum and H. G. Jung, "Enhancing light blob detection for intelligent headlight control using lane detection," *IEEE Transactions on Intelligent Transportation Systems*, vol. 14, no. 2, pp. 1003–1011, 2013.
- [4] D. Jurić and S. Lončarić, "A method for on-road night-time vehicle headlight detection and tracking," in *2014 International Conference on Connected Vehicles and Expo (ICCVEx)*, 2014, pp. 655–660.
- [5] P. Sevekar and S. B. Dhonde, "Nighttime vehicle detection for intelligent headlight control: A review," in *Proceedings of the 2016 2nd International Conference on Applied and Theoretical Computing and Communication Technology (iCATccT)*, 2016, pp. 188–190.
- [6] R. K. Sazoda and M. M. Trivedi, "Looking at vehicles in the night: Detection and dynamics of rear lights," *IEEE Transactions on Intelligent Transportation Systems*, vol. 20, no. 12, pp. 4297–4307, 2019.
- [7] C. J. Rapson, B.-C. Seet, M. A. Naem, J. E. Lee, M. Al-Sarayreh, and R. Klette, "Reducing the pain: A novel tool for efficient ground-truth labelling in images," in *2018 International Conference on Image and Vision Computing New Zealand (IVCNZ)*, 2018, pp. 1–9.
- [8] E. Oldenziel, L. Ohnemus, and S. Saralajew, "Provident detection of vehicles at night," in *2020 IEEE Intelligent Vehicles Symposium (IV)*, 2020, pp. 472–479.
- [9] S. Ren, K. He, R. Girshick, and J. Sun, "Faster R-CNN: Towards real-time object detection with region proposal networks," in *Advances in Neural Information Processing Systems* 28, 2015, pp. 91–99.
- [10] F. M. Naser, "Detection of dynamic obstacles out of the line of sight for autonomous vehicles to increase safety based on shadows," Master's thesis, MIT, Boston, 2019.
- [11] A. Borji and L. Itti, "CAT2000: A large scale fixation dataset for boosting saliency research," *arXiv:1505.03581 [cs.CV]*, 2015.
- [12] L. Itti and A. Borji, "Computational models: Bottom-up and top-down aspects," *arXiv:1510.07748 [cs.CV]*, 2015.
- [13] J. Zhang and S. Sclaroff, "Saliency detection: A boolean map approach," in *2013 IEEE International Conference on Computer Vision*, 2013, pp. 153–160.
- [14] A. Borji, M. Cheng, H. Jiang, and J. Li, "Salient object detection: A benchmark," *IEEE Transactions on Image Processing*, vol. 24, no. 12, pp. 5706–5722, 2015.
- [15] T. R. Singh, S. Roy, O. I. Singh, T. Sinam, and K. M. Singh, "A new local adaptive thresholding technique in binarization," *IJCSI International Journal of Computer Science Issues*, vol. 8, no. 6, pp. 271–277, 2011.
- [16] L. Ewecker, E. Asan, L. Ohnemus, and S. Saralajew, "Provident vehicle detection at night for advanced driver assistance systems," *arXiv preprint arXiv:2107.11302 [cs.CV]*, 2021.
- [17] T.-Y. Lin, M. Maire, S. Belongie, J. Hays, P. Perona, D. Ramanan, P. Dollár, and C. L. Zitnick, "Microsoft COCO: Common objects in context," in *European Conference on Computer Vision*. Springer, 2014, pp. 740–755.
- [18] S.-E. Wei, V. Ramakrishna, T. Kanade, and Y. Sheikh, "Convolutional pose machines," in *Proceedings of the IEEE Conference on Computer Vision and Pattern Recognition (CVPR)*, 2016, pp. 4724–4732.
- [19] K. Sun, B. Xiao, D. Liu, and J. Wang, "Deep high-resolution representation learning for human pose estimation," in *Proceedings of the IEEE/CVF Conference on Computer Vision and Pattern Recognition (CVPR)*, 2019, pp. 5693–5703.
- [20] F. Zhang, X. Zhu, H. Dai, M. Ye, and C. Zhu, "Distribution-aware coordinate representation for human pose estimation," in *Proceedings of the IEEE/CVF Conference on Computer Vision and Pattern Recognition (CVPR)*, 2020, pp. 7093–7102.
- [21] A. Paszke, S. Gross, F. Massa, A. Lerer, J. Bradbury, G. Chanan, T. Killeen, Z. Lin, N. Gimelshein, L. Antiga, A. Desmaison, A. Kopf, E. Yang, Z. DeVito, M. Raison, A. Tejani, S. Chilamkurthy, B. Steiner, L. Fang, J. Bai, and S. Chintala, "PyTorch: An imperative style, high-performance deep learning library," in *Advances in Neural Information Processing Systems* 32, 2019, pp. 8024–8035.

APPENDIX I
BOUNDING BOX ANNOTATION CONSISTENCY

Usually, BB annotations created by experts for object detection can be considered as objective ground truth. However, for instances, this ground truth is subjective. To study this subjectiveness, we compared the BB annotations for direct and indirect instances across several annotators. The results confirm the following hypothesis: *BB annotations vary to a not negligible extent between different annotators or even for the same annotator between different frames.*

A. Experiment Setup

To study the annotation consistency, seven experts were tasked to annotate the same scene with BBs. Thereby, the annotation inconsistency that might be observed is two-fold: First, some experts might decide to not annotate an instance because it is too weak or cannot be separated from another instance. Second, after the experts agreed on the existence of an instance, the actual size and position of the BB are also subject to the subjective behavior of the annotators.

We decided to only study the subjectivity of the BB placement. This decision was made to reduce the evaluation complexity of the experiment while still emphasizing the overall problem. This led to the following experiment setup:

- 1) Two instances (one direct, one indirect) were selected for annotation. The participants were shown an example image to clarify the annotation targets.
- 2) The experts annotate the scene (number 15) from start to end using BBs.
- 3) The resulting annotations are evaluated with appropriate metrics.

B. Evaluation Metrics

For evaluation, annotated BBs were collected from all N experts. To explain the evaluation scheme, we will focus on the consistency of all BBs $B = \{b_1, \dots, b_N\} = \{(\mathbf{p}_{1,1}, \mathbf{p}_{1,2}), \dots, (\mathbf{p}_{N,1}, \mathbf{p}_{N,2})\}$ for an instance in one frame. Metrics are calculated for the direct and indirect instances separately and then averaged over all frames. A BB is described by its upper-left corner $\mathbf{p}_{i,1}$ and its lower-right corner $\mathbf{p}_{i,2}$. $\text{Rect}(b_i)$ defines the set of all points inside the BB b_i . Drawing from common object detection metrics, the IoU can be used to compress the position and size variations of BBs into a scalar value. This is usually done by comparing a predicted BB to a ground truth BB. Since this is not applicable for our purpose, we compare the expert annotations to the mean BB \bar{b} , specified as the average over all annotations:

$$\bar{b} = (\bar{\mathbf{p}}_1, \bar{\mathbf{p}}_2) = \left(\frac{1}{N} \sum_{i=1}^N \mathbf{p}_{i,1}, \frac{1}{N} \sum_{i=1}^N \mathbf{p}_{i,2} \right).$$

Using this as a reference, the IoU values to all BBs are calculated:

$$\text{IoU}(b_i, \bar{b}) = \frac{|\text{Rect}(b_i) \cap \text{Rect}(\bar{b})|}{|\text{Rect}(b_i) \cup \text{Rect}(\bar{b})|}.$$

Assuming, that all annotations are drawn from the same distribution, we can infer the statistics and therefore the

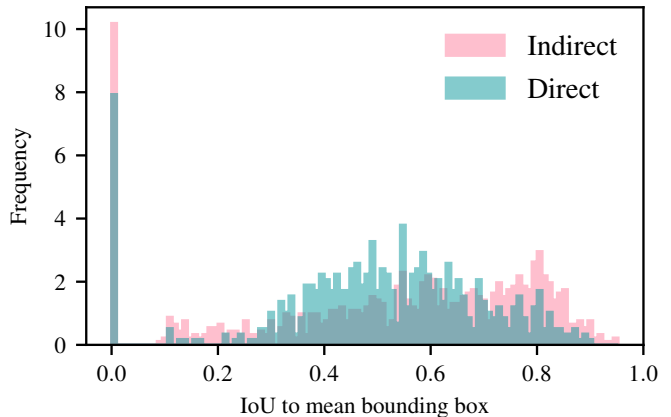


Fig. 5. Histogram of IoU values cumulated over all frames.

consistency of the expert annotations. If annotators choose not to annotate the instance, an IoU of zero is assigned. Therefore, we expect outliers from the distribution and will use the median IoU as a representative average metric. For optimal annotations, the distribution will collapse to a Dirac distribution with unit mean.

C. Results

The results shown in Fig. 5 support our hypothesis, that a consistent, manual annotation with BBs is not possible. Here, the abundance of missing annotations (mainly caused by different starts and ending frames) shows, that even for a specified image region, the experts could not agree on a consistent ground truth. Interestingly, the direct annotations suffered from more inconsistency than the indirect instance. We think, that this is mainly due to the big glare area surrounding the instance, leading the experts to largely different BB sizes. It is safe to say, that this inconsistency will cause problems for systems learning from this ground truth data. Basically, each new annotator introduces a domain shift into the annotations, which makes it quite difficult to work with.

TABLE III
CLASSIFIER ARCHITECTURE OF THE CUSTOM MODEL.

Layer	Input channels	Output channels	Kernel size	Stride
Conv2D + ReLU	1	32	5	1
Conv2D + ReLU	32	64	3	1
MaxPool2D	64	64	2	2
BatchNorm2D	64	64	-	-
Conv2D + ReLU	64	64	5	1
Conv2D + ReLU	64	128	3	1
MaxPool2D	128	128	2	2
BatchNorm2D	128	128	-	-
Conv2D + ReLU	128	128	5	1
Conv2D + ReLU	128	256	3	1
AvgPool2D	256	256	5	1
BatchNorm2D	256	256	-	-
Linear + ReLU + Dropout	256	128	-	-
Linear + ReLU	128	64	-	-
Linear + Sigmoid	64	1	-	-